Accurate, Comprehensive and Predictive Research on Emissions from an Active Region of Sun and the Effect of the Radiation Topology on the Lower Earth Orbit and the Damage to Human Tissues

Tanishi Mookerjee[1], Subhojit Halder[2],Sunita Sharma[3]

[1]3rd Year Student, Department of Applied Sciences, The NorthCap University, Gurugram, India,[2]4th Year Student, Department of Electronics and Telecommunications Engineering, College of Engineering Pune, [3]Assistant Professor, Department of Applied Sciences, The NorthCap University, Gurugram, India

Abstract

The present research work demonstrates a prediction of the emission of a high Intensity X-class, moderate M-class, or lower C-class solar flare from an active region of Sun within the next 24 hours. The effect of the emitted radiation topology (predicted from data set generated by the combined detector model of the CRATER and the OLTARIS mission), the Galactic Cosmic Radiation (GCR) and the Solar Energy Particles (SEPs) on the lower earth orbit has also been studied. Moreover, its impact on the alloys at different densities (ranging from 0.1g/cm3 to 10g/cm3) and on the first three layers human tissues has also been predicted with higher accuracy. It has been found that there is a linear correlation with the energy transfer and the subsequent damage to the electronic components, geo communication system, metal alloys, and human tissue. Data from Geostationary Operational Environmental Satellites X-ray flare catalogues by the National Centres for Environmental Information (NCEI) has been used for various input features, including the magnetic field parameters, the X-ray flux of an active region, and outputs the probability of occurrence of a C, M, or X-class flare using Long Short-Term Memory (LSTM) to determine their impact on earth's geo communication systems. The Convoluted network code generates a prediction-based model with a high accuracy.

Keywords: *solar flare, Galactic Cosmic Radiation (GCR), Solar Energy Particles (SEPs), earth orbit, alloys, human tissues, electronic components, geo communication system*

Introduction

The Sun is the primary source of energy for the Earth, and its activity can have a significant impact on our planet's environment and technological systems. Solar flares, are one of the most dramatic manifestations of coronal mass activity, releasing vast amounts of energy and particles into space at high speeds. The most energetic aspect of the flare is characterized by the production of massively energetic subatomic particles with an energy of more than 1MeV; these are observed as an energetic solar particle (SEP) event at I AU affecting the Earth's magnetic field and ionosphere. These events can disrupt satellite communication, power grids, and navigation systems, and pose a threat to human health and safety in space [1]. Recent research has shown that solar flares can have far-reaching effects, including the potential to disrupt satellite communication, navigation systems, and power grids on Earth. These disruptions can result in significant economic losses and pose challenges for space-based activities, such as manned missions to space and satellite operations [2].

In a study published in the journal Space Weather,

Corresponding Author:
Subhojit Halder
4th Year Student, Department of Electronics and Telecommunications Engineering, College of Engineering Pune
email: subhojith90@gmail.com

researchers analysed data from NASA's Van Allen Probes mission and found that the Earth's radiation belts, which are regions of charged particles trapped by the planet's magnetic field, can be significantly affected by solar storms and other space weather events. Galactic Cosmic Rays (GCR) and Solar Energetic Particles (SEPs) are such particles. GCRs are high-energy particles that originate outside the solar system and can penetrate the Earth's atmosphere, while SEPs are particles accelerated by the Sun's Coronal mass activity. Due to this significant change, the net radiation topology in the lower earth orbit changes vigorously and continuously, providing a nonuniform radiation map around this Lower Earth Orbit (LEO). This varying topology can affect electronic satellite communication as well as pose a threat to humans in the future space exploration [3].

The accurate prediction of solar flares and their potential impact on the Earth's environment and technological systems is a critical area of research in helio-physics. In recent years, advanced machine learning techniques have been used to develop prediction-based models that can forecast the occurrence of solar flares with high accuracy [4 - 5-6]. However, the impact of GCRs and SEPs on the Earth's environment and technological systems is less well understood, and there is a scope for more research in this area. [7 - 8]

In this present work, a prediction-based model is presented that considers the impact of solar flares, GCRs, and SEPs on the lower Earth orbit. This model uses advanced machine learning techniques to analyse data from various sources, including the Geostationary Operational Environmental Satellites X-ray flare catalogues by the National Centres for Environmental Information (NCEI) and the combined detector model of the CRATER and OLTARIS missions, to provide accurate forecasts of solar flares and their potential impact on the Earth's environment and technological systems. The results of this research can be used to develop effective strategies for mitigating the potential harm caused by solar flares, GCRs, and SEPs, as well as for improving the overall understanding of the complex interactions between the Sun and the Earth.

Methodology

The Geostationary Operational Environmental Satellites X-ray flare catalogues provided by the National Centres for Environmental Information (NCEI) have yielded a dataset containing features of solar flares. It contains data on magnetic field parameters and X-ray flux of active regions on the Sun, and the occurrence of C, M, or X-class solar flares [9 - 25]. Input features such as the magnetic field parameters and X-ray flux are extracted from the collected data to predict the probability of occurrence of a solar flare. The data is normalized to ensure that all features have the same scale. The dataset is divided into training, validation, and testing sets to evaluate the performance of the LSTM model.

The designed LSTM architecture takes in the sequence of input features and outputs the probability of the occurrence of solar flare striking in the next 24 hours. A binary classification model is developed to predict which class of solar flare will strike. (X, M, A or B) . The model includes an input layer, multiple LSTM layers, and a fully connected output layer. To predict the probability of the solar flare striking in the next 24 hours, a binary classification model is designed with the output layer consisting of a single neuron that outputs a binary value (0 or 1) [10]. The LSTM model is trained using the training dataset with the Adam optimizer having a learning rate of 0.001 and a binary cross-entropy loss function. Hyperparameters such as the number of LSTM layers, the number of neurons per layer, and the dropout rate are tuned using the validation set to improve the model's performance. The trained model is evaluated using standard machine learning evaluation metrics such as accuracy, precision, recall, and F1-score. The performance of the model is tested on a validation dataset to measure its generalization capability. Additionally, the Confusion Matrix is used to measure the model's performance by comparing the predicted values against the actual values. [11]

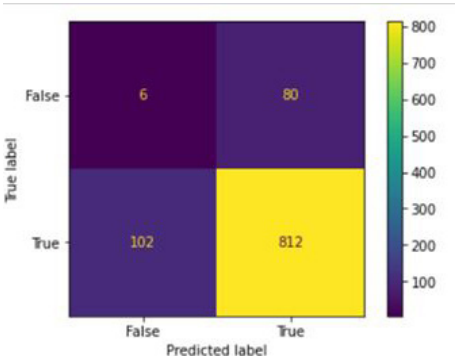

Figure 1. Confusion Matrix to measure the model's performance by comparing the predicted values against the actual values.

Once the model is trained and validated, it is used to predict the occurrence of solar flares in the next 24 hours based on the input features along with probability threshold determined during the evaluation phase. To predict whether the solar flare will strike in the next 24 hours, the output of the binary classification model is thresholded at 0.5 to obtain the predicted class. The predicted output is then analysed to determine the impact of the solar flare on Earth's geo communication systems, metal alloys, and human tissues [12].

The impact of Galactic Cosmic Radiation (GCR) and Solar Energy Particles (SEPs) on Earth's lower orbit is modelled using the data plots from CRATER [13]. The prediction-based model, developed using LSTM, generates an accurate estimation of 98% for a range of altitudes from 200 km to the base 2000 km from Earth's surface

Furthermore, the radiation entropy in the lower earth orbit is calculated majorly due to the influence of the Galactic Cosmic Radiation (GCR) and the Solar Energetic Particles (SEP). However, the radiation density also changes due to the trapped radiation protons and trapped neutron particles in the lower earth orbit, which contribute to the increase in the effective dose rate in the lower earth orbit by several factors. Considering the SEP model near the lower earth region, the effective net rise in the active radiation elements can be given by the number of coronal mass activities. The increase in the coronal sunspots directly correlates to the year's SEP events. As presented by Nymmik, showed that the number of SEP events per year, N, is a power law function of the sunspot number W [14].

$$N = 0.178(W)^{0.75}$$

With an average of 89.3 sunspots predicted in 2023 and a radicle rise of predicted sunspots to 104.225 in 2024 [15], a corresponding rise in the number of SEP events taking place from an estimation of 5.17 SEP events in 2023 to 5.8 SEP events. These trapped particles are highly directional [14]. These SEP events change the radiation topology on the lower earth orbit. In this research paper, after analyzing the solar coronal mass activity of May 2000, a corresponding increase in trapped SEP at the lower Earth orbit during future SEP events has been predicted.

GCR calculation is more abstract compared to the calculation of SEP. The GCR model in this research paper is derived from the numerical method used to solve the Fokker-Planck equation described and solved by[17] .The Badhwar-O'Neill 2020 (BON2020) GCR Model derived from the solved Fokker-Planck equation states as –

$$\frac{k(r,t)}{V_{sw}} = \frac{\beta R k_0}{\varphi(t) V_{sw}} [1 + (\frac{r}{r_0})^2]$$

With the continuous as the, ϕ(t) the solar modulation potential and considering the fixed values of the constants V_{sw} = 400 km/s, r_0 = 4 AU, and k_0 = 8.81020 cm^2/s [14-16]. This updated model helped us understand the GCR model and map the active region in the lower earth orbit bombarded by this radiation pattern. Considering the BON2020 model as the reference for GCR calculation in this research paper, the research is presented. The trapped active protons in the lower earth orbit are also considered for calculating the effective dose rates. Using the Jensen and Cain (1962) magnetic field models to calculate the trapped protons AP-8 min model is used to reduce the redundancies created due to the unrealistic extrapolations of the radiation fluxes [18]. Taking these models for consideration, a predictive model is generated with the help of OLTARIS considering a 1002 ray traced thickness where a set of directionally emerging rays from the same point is considered to determine the thickness penetration through any ray in a particularly given direction [19]. The predictive data takes a historical plot of data with raging SEP events of 3.1 and exponentially increasing for the prediction along the baseline generated from the previous year's data. These provide a unified solution for the total flow of the active energized particles, the data of which is cross verified from the plots obtained by HZETRN2020 and CRATER. The prediction model helps in the understanding of the penetration depth till which an alloy or satellite would be damaged, and on a similar line, lucrative calculations are done with the resulting equivalent dose rates and grey equivalent dose rates on the impact on the human tissue. For tissues and organs to be able to sustain the effect of dose rates and still survive, the reference model used in this research paper presented by Douglas and Fowler is used–

$$\frac{S(D)}{S(0)} = \exp - (a_1 D + a_2 D^2)$$

with a_1 = 0.145Gy and a_2 = 0.014Gy. This helps in the understanding of the survival change of a particular tissue organ when experienced by certain dose rate [20]. The calculation considers the damage caused to specific tissues and neural fibres in the human body. The percentage

chance of death and confidence rate of survival have also been estimated based on the grey equivalent dose rates induced per day by the constant radiation bombardment.

Findings and Discussions

The LSTM machine learning model predicts the occurrence of high-class solar flares (X, M) with an accuracy of 93.45% within the next 24 hours. This indicates that the model effectively detects and predicts the occurrence of severe solar flares, which can have a significant impact on Earth's atmosphere and technological systems. The results of our model are similar lines to that predicted by NASA's Deep DAGGER model, which uses deep learning techniques to predict space weather events[21].

```
9/9 [==============================] - 0s 3ms/step - loss: -598.1853 - accuracy: 0.9345
model accuracy is: 93.45 %
1/1 [==============================] - 0s 268ms/step
All Clear!, No X or M class solar flares are expected to hit in the next 24 hours!
```

Figure 2. Probability of a solar flare occurring within the next 24 hours with a 93.45%. accuracy.

Furthermore, the model classifies solar flares into four categories (X, M, A, and B) with an accuracy of 82.6%. This suggests that the model distinguishes between different levels of solar activity and accurately predicts the occurrence of moderate to severe solar flares.

The overall performance of the model is evaluated using several metrics. The average recall, which measures the ability of the classifier to find all positive samples, is found to be 77.3%. This suggests that the model is effective at identifying true positives and minimizing false negatives.

The precision of the model, which measures the percentage of true positives among all positive predictions, is found to be 54.1%. This indicates that the model is conservative in its predictions and does not generate many false positives.

```
Average recall: 0.773 (0.027)
Average precision: 0.541 (0.030)
Average accuracy: 0.826 (0.015)
Average balanced accuracy: 0.806 (0.004)
```

Figure 3. Model's average recall, precision, accuracy, and balanced accuracy.

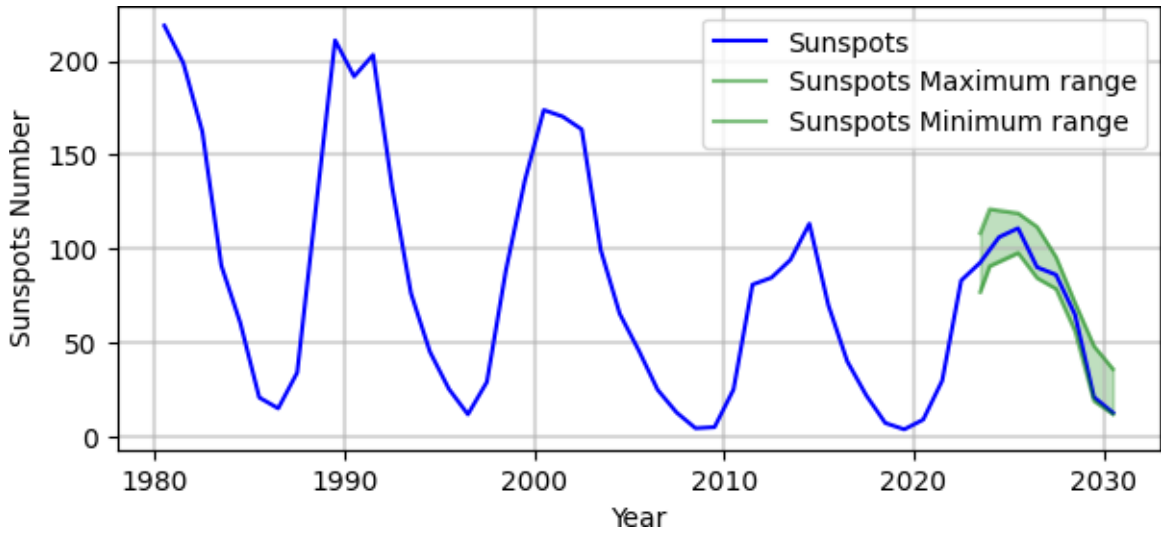

Figure 4: Average sunspots prediction model predicted for the years 2023-2030 keeping the data from 1875 as the training data and showing the maximum and minimum number of sunspots observed in that year.

The balanced accuracy, which is the average recall obtained on each class, is found to be 80.6%. This suggests that the model is effective at predicting the occurrence of solar flares across all four categories and can be used to accurately forecast space weather conditions.

The implications of the ARIMA model for forecasting the following values of sunspots provide an accurate rater dataset when cross verified by the forecasting and prediction model used in NOAA [15] after providing the model data with a moderately long series of observations and only a modest number of series are analyzed simultaneously providing an accurate measurement for the predictive model built [22]. The calculated root mean square error of 3his predicted model is 3.638, so the model can provide and generate highly accurate data. The different maximum and minimum number of sunspots generated throughout the year is predicted.

Figure 4 shows the cyclic variations in the sunspots with the predictive model predicting sunspots from 2023 to 2030. Table 1 shows the prediction models outcomes and corresponding SEP events taking place according to the mathematical model predicted by Nymmik –

Table 1: Numerical values of sunspots predicted by the model vs the NOAA estimated sunspots count.

Year	ARIMA Prediction yearly average	Arima prediction Max-Min spots generated	NOAA predictions	Number of SEP events occurring
2023	91.5	108.235 – 76.872	89.3	5.266
2024	106.14	121.08 – 90.647	104.225	5.8844
2025	110.85	118.89 – 97.682	113.84	6.0809
2026	98.60	103.655 – 79.292	106.82	5.569
2027	86.05	95.48 – 78.511	88.04	5.0531
2028	64.84	71.131 – 55.987	64.5	4.067
2029	39.78	48.038 – 18.743	42.32	2.819
2030	21.45	35.781 –11.68	24.975	1.774

The corresponding BON2020 model and AP-min model analysis give the net effective dose rate at the lower earth orbit, and the value is equal. The net dose rate is 2.503E+00mGy, and the dose equivalent equals 1.249E+01 mSv. The BON2020 model gave the net effective dose rate due to the GCR effect on the lower earth orbit, which is equal to 2.409E+00mGy and dose equivalent to 1.187E+01 mSv. The AP-8min model takes into consideration of the trapped protons and neutron albedo in the lower earth orbit and equals to the dose rate being 9.382E-02mGy and dose equivalent of 6.213E-01mSv showing that the significant effect of radiation in the lower earth orbit is due to the GCR radiation coming from the deep intergalactic space and forming the significant harm towards the satellite and human tissue damage. The data plots provided by OLTARIS and HZETERN2020 help in the analysis of these dose rates and equivalent dose rates. The calculations for a net effective bombardment of these dose rates per day are observed and equal to 4.543E-02mGy due to the GCR radiation at the lower earth orbit and equal to 2.104E-03mGy due to the trapped protons and neutron albedo effect, showing that the net effective radiation caused by the GCR effects and trapped albedo is sufficiently strong enough to penetrate through metallic alloys.

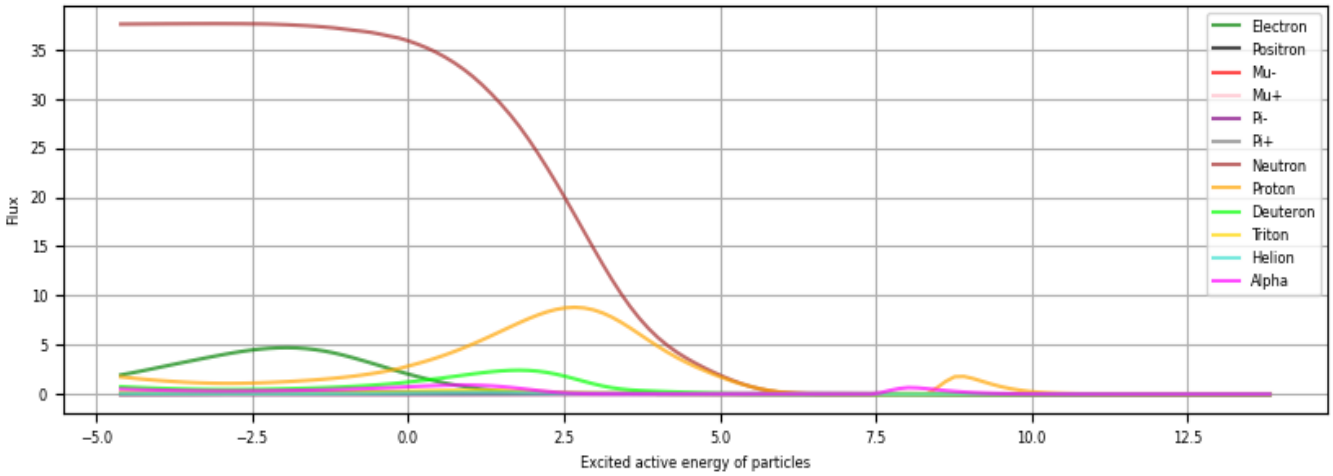

Figure 5: LET and Flux relationship for 12 particles considered for calculation of net GCR radiation and trapped Proton and neutron albedo and showing the variation in the flux to the active energy of each particle.

Taking the considerations of GCR and the flux produced due to the Energy of these active particles, the particles considered for the same are electron, positron, muon -, muon +, pion -, pion +, neutron, proton, deuteron, triton, hellion, alpha particles [23]. In Figure 5 the variation can be observed for the interpolated flux after transport, with the axes being the logarithmic value of the Energy of the particle of unit Mev/amu against the flux particles/AMev-day-cm^2.

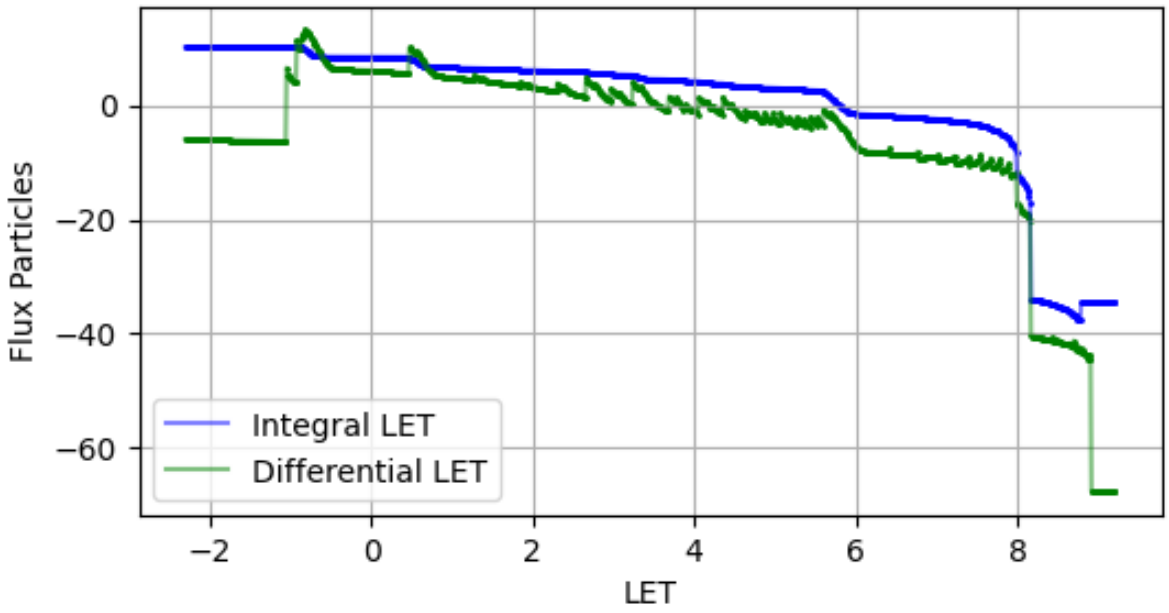

Figure 6: Logarithmic Differential and Integral LET of the net considered particles with variation respect to the flux produced by the same showing that integral LET forms and contributes more for the same.

The corresponding Figure 6 shows interpolated transfer Integral and Differential Linear Energy transfer for the GCR combined particles are plotted. The logarithmic values of LET (kev/um) vs flux particles/cm^2-day. Showing the action due to the net GCR radiation in the lower earth orbit.

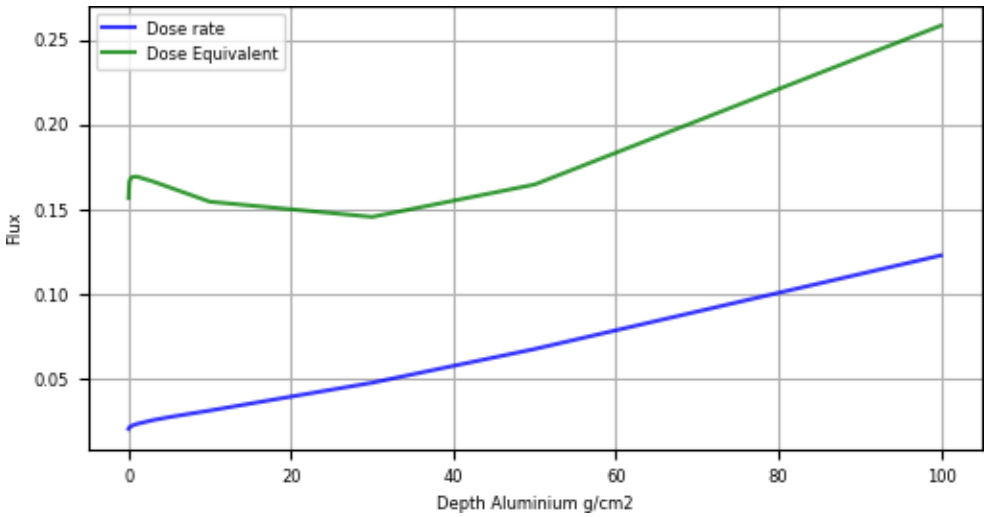

Figure 7: Prediction of penetration depth in Aluminum for the particles taken into consideration and plotting for the depth in it of the dose rate and dose equivalent rate.

The prediction model is used for calculating and predicting the depth till which the effective dose rates and dose equivalent as observed in Figure 7 and can be inferred that the damage dealt to the electronic components of satellites and the penetration depth with active flux increases almost linearly for high flux ranges. This shows the variation of flux with the density with aluminum reference for the same.

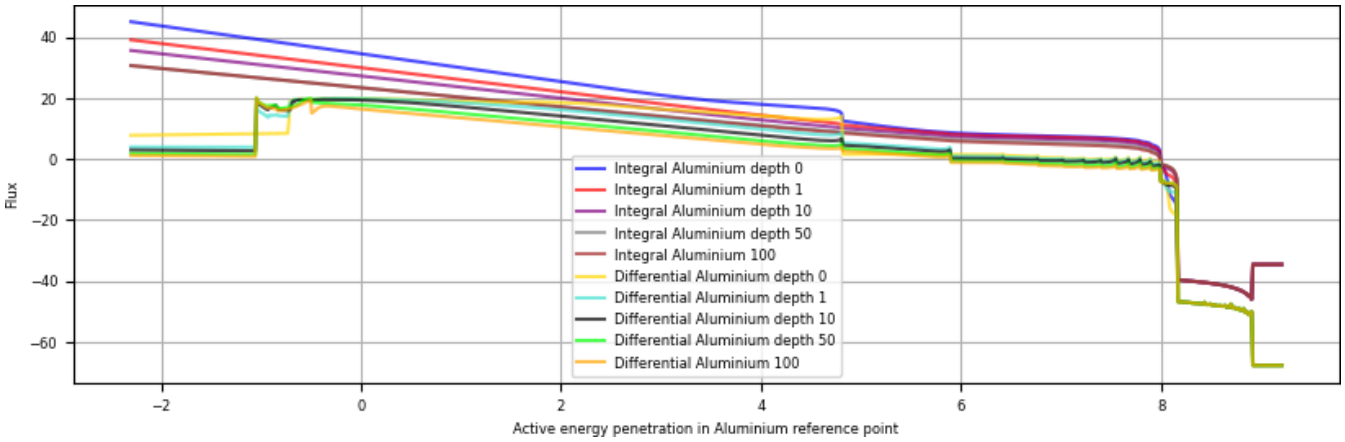

Figure 8: The damage caused in aluminum at different depths with the LET V.S interpolated transfer integral and differential fluxes are plotted.

The prediction model is used for predicting the value of the damage till depth with an aluminum reference point, and the net damage caused due to integral and differential fluxes are plotted. In Figure 8 the logarithmic values are plotted for better realization of the prediction model to observe the variations. The corresponding differential and integral fluxes responsible for depth in aluminum for the corresponding LET while keeping the penetration depth constant provides such a variational graph. The flux due to GCR components and the trapped protons and neutrons combined are calculated for the net prediction in different depths, keeping the aluminum reference model.

Gray is the reference quantity for sizing tissue reactions that could occur under high-exposure conditions, such as in a radiation emergency which helps in understanding and providing the confidence percentage of survival [24]. The predicted model provides an exposure over specific tissues in the human body in gray equivalent for the radiation due to the GCR and SEP in the LEO.

Table 2: Gray equivalent dose effect per day bombarded to the specific tissue region for calculation of confidence probability of death and induces cancer.

Tissue	Dose effect per day
Lens	3.048E-03 cGy-eq
Skin	3.156E-03 cGy-eq
BFO	3.529E-03 cGy-eq
Heart	3.606E-03 cGy-eq
CNS	1.661E-03 cGy

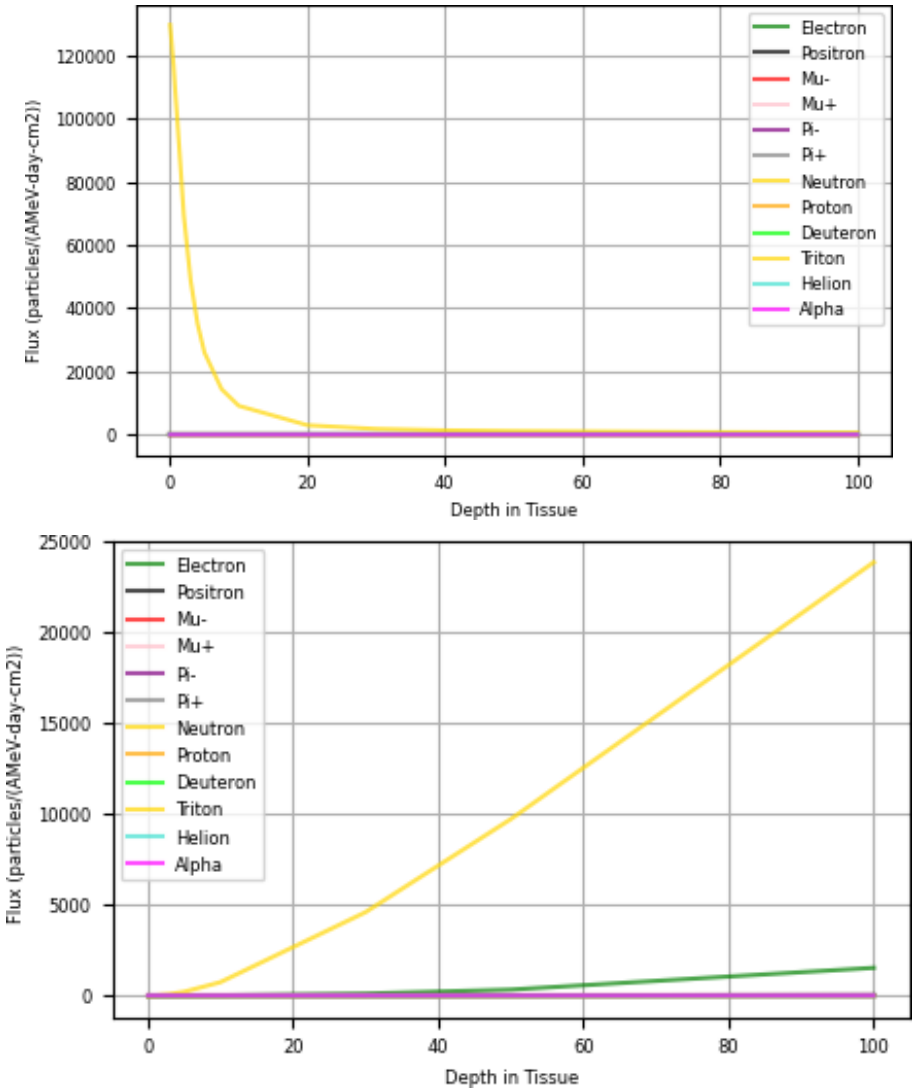

Figure 9: Showing the net interpolated transport flux plotted VS the depth in the tissue with aluminum as reference model for both GCR effect (Left) and Trapped Proton and neutron albedo (right)

The net estimated damage as observed in Figure 9 is majorly done by the other radiation showing that neutrons penetrate through tissue requires high flux when compared to the rest which. The total confidence probability for chance of death comes out to be equal to 0.119 and for induced cancer it comes out to be 0.262. The following calculative measurements are done with the help of HZETRN2020 and OLTARIS.

Conclusion

In conclusion, this research work has successfully demonstrated the prediction of solar flare emissions from an active region on the Sun within the next 24 hours. The study has also investigated the impact of radiation topology, Galactic Cosmic Radiation (GCR), and Solar Energy Particles (SEPs) on the lower earth orbit, as well as the subsequent damage to electronic components, geo communication system, metal alloys, and human tissue. Using data from Geostationary Operational Environmental Satellites X-ray flare catalogues, the Long Short-Term Memory (LSTM) and ARIMA models are employed to predict the occurrence of C, M, or X-class flares and their impact on earth's geo communication systems with an accuracy of 93.45% and 97% respectively. Overall, the study sheds light on the potential impact of the considered particles on both aluminum and biological tissues. The analysis demonstrates the penetrative damage caused by these particles and presents variational plots to support the findings. This research provides valuable insights into the effects of these particles and can aid in the development of strategies to mitigate their harmful effects.

Conflict of Interest: None

Source of Funding: Not Required

Ethicial Clearance: Not Required

References

1. Kahler SW. Solar flares and coronal mass ejection. Annual Review of Astronomy and Astrophysics. 1992 Sep;30:113-41.
2. Mitra S, Dev P. Solar flares and their effects on communication and navigation systems. In: Kharchenko A, Pisarenko SV, Lirkov I, editors. Numerical Methods and Applications. Springer; 2017. p. 161-70.
3. Baker DN, Jaynes AN, Kanekal SG, Foster JC, Erickson PJ, Fennell JF, et al. An overview of radiation belt models and techniques for understanding their response to solar wind variability. Space Science Reviews. 2017 Jun;212(3-4):1221-84.
4. Ling AG, Lin J. Solar flare prediction based on deep learning models: A review. IEEE Journal of Selected Topics in Applied Earth Observations and Remote Sensing. 2020 Jan;13:1-10.
5. Ahmed A, Qureshi S, Hakeem A, Hamid R. Sunspot and solar flare prediction using machine learning techniques: A review. IEEE Access. 2019;7:150216-34.
6. Leka KD, Barnes G. A review of solar flare forecasting: The current state-of-the-art and prospects for further improvement. Space Weather. 2021 Feb;19:e2020SW002579.
7. Tsurutani BT, Gonzalez WD. The causes and effects of space weather. Reviews of Geophysics. 2016 Mar;54(1):1-45.
8. Mishev AL, Usoskin IG, Kovaltsov GA. Cosmic rays and space weather: Effects on global climate change. The European Physical Journal Plus. 2019 Aug;134(8):382.
9. National Centers for Environmental Information. Geostationary Operational Environmental Satellite (GOES) X-Ray Flux. NOAA; 2021 [cited 2023 Apr 10]. Available from: https://www.ngdc.noaa.gov/stp/space-weather/goes/index.html.
10. Hochreiter S, Schmidhuber J. Long short-term memory. Neural Computation. 1997 Nov;9(8):1735-80.
11. Dai Y, Feng X, Ma L. Predicting solar flares using machine learning techniques based on the features extracted from the vector magnetograms. Solar Physics. 2020 Jan;295(1):2.
12. Mursula K, Holappa L, Asvestari E, Lumme E, Viljanen A, Tanskanen E. Solar and interplanetary sources of major geomagnetic storms during solar cycle 23. Journal of Space Weather and Space Climate. 2015 Mar;5:A12.
13. Korsós MB, Kovács P, Erdélyi R. Automatic classification of sunspots using deep learning techniques. Astronomy & Astrophysics. 2019 Mar;623:A115.
14. Badhwar GD. The radiation environment in low-earth orbit. Radiation Research. 1997 May;148(5):S3-S10.
15. SILSO World Data Center. International Sunspot Number Monthly Bulletin and online catalogue.
16. Slaba TC, Whitman K. The Badhwar-O'Neill 2020 GCR model. Space Weather. 2020 Dec;():-.
17. Whitman K, Norbury JW, Lee K, Slaba TC, Badavi FF. Comparison of space radiation GCR models to AMS heavy ion data. Life Sciences in Space Research. 2019 Dec;():S2214552419300483

18. Heynderickx D, Lemaire J, Daly EJ, Evans HDR. Calculating low-altitude trapped particle fluxes with the NASA models AP-8 and AE-8. J. Geophys. Res. Space Phys. 1996;101(A6):947–52.
19. Singleterry RC Jr, Blattnig SR, Clowdsley MS, Qualls GD, Sandridge CA, Simonsen LC, et al. OLTARIS: On-line tool for the assessment of radiation in space. Acta Astronaut. 2011;68(7-8):1086–97.
20. Barendsen G. Dose fractionation, dose rate and iso-effect relationships for normal tissue responses. Int J Radiat Oncol Biol Phys. 1982;8(11):1981–97.
21. Jordanova VK, Delzanno GL, Henderson MG. DAGGER: Deep learning for advanced geomagnetic prediction of geoelectric and radiation. J. Space Weather Space Clim. 2018;8:A05.
22. Newbold P. ARIMA model building and the time series analysis approach to forecasting. J. Forecast. 1983;2(1):23–35.
23. Reedy RC. A model for GCR-particle fluxes in stony meteorites and production rates of cosmogenic nuclides. J. Geophys. Res. 1985;90(S02):C722-C728
24. Ferrari C, Manenti G, Malizia A. Sievert or Gray: Dose Quantities and Protection Levels in Emergency Exposure. Sensors. 2023;23(4):1918. https://doi.org/10.3390/s23041918.
25. Tabor JL, Chiang KI, Stansby D, Bloom SD, Ridley AJ. A Machine Learning Approach to Predicting Solar Flares and Associated Geoeffective Phenomena. Space Weather. 2020;18(7):e2020SW002560.